Published in final edited form as:

Dev Biol. 2016 April 15; 412(2): 208–218. doi:10.1016/j.ydbio.2016.01.042.

Coiled-coil domain containing 42 (Ccdc42) is necessary for proper sperm development and male fertility in the mouse

Raymond C. Pasek[a], **Erik Malarkey**[a], **Nicolas F. Berbari**[b], **Neeraj Sharma**[a], **Robert A. Kesterson**[c], **Laura L. Tres**[d], **Abraham L. Kierszenbaum**[d], and **Bradley K. Yoder**[a,*]

[a]Department of Cell, Developmental and Integrative Biology, University of Alabama at Birmingham, Birmingham, AL USA

[b]Department of Biology, Indiana University-Purdue University Indianapolis Indianapolis, IN USA

[c]Department of Genetics, University of Alabama at Birmingham, Birmingham, AL USA

[d]Department of Cell Biology and Anatomy, The Sophie Davis School of Biomedical Education; The City University of New York; New York, NY USA

Summary

Spermiogenesis is the differentiation of spermatids into motile sperm consisting of a head and a tail. The head harbors a condensed elongated nucleus partially covered by the acrosome-acroplaxome complex. Defects in the acrosome-acroplaxome complex are associated with abnormalities in sperm head shaping. The head-tail coupling apparatus (HTCA), a complex structure consisting of two cylindrical microtubule-based centrioles and associated components, connects the tail or flagellum to the sperm head. Defects in the development of the HTCA cause sperm decapitation and disrupt sperm motility, two major contributors to male infertility. Here, we provide data indicating that mutations in the gene *Coiled-coil domain containing 42* (*Ccdc42*) is associated with malformation of the mouse sperm flagella. In contrast to many other flagella and motile cilia genes, *Ccdc42* expression is only observed in the brain and developing sperm. Male mice homozygous for a loss-of-function *Ccdc42* allele (*Ccdc42*^{KO}) display defects in the number and location of the HTCA, lack flagellated sperm, and are sterile. The testes enriched expression of *Ccdc42* and lack of other phenotypes in mutant mice make it an ideal candidate for screening cases of azoospermia in humans.

Keywords

sperm; infertility; sperm head-tail coupling apparatus; Ccdc42; intramanchette transport

*Corresponding Author: Bradley K. Yoder, Ph.D., Department of Cell, Developmental and Integrative Biology, 1918 University Blvd., Birmingham, AL 35294. Tel.: (205) 934-0995; FAX: (205) 934-0990., byoder@uab.edu.

Introduction

Impaired fertility is common among the general human population, occurring in about 1 in 20 men of reproductive age and is frequently due to reduced sperm motility and structural defects (De Kretser and Baker, 1999; Holden et al., 2005). To understand the biology of reproduction and the causes of these reproductive deficits, it is essential that genes required for sperm development, maturation, and motility be identified and their molecular functions be assessed (Borg et al., 2010).

Spermatogenesis is a complex process characterized by sequential morphological changes in the seminiferous tubules initiated during puberty. At this time, spermatogonia cease mitotic proliferation and become primary spermatocytes that are committed to undergo two consecutive meiotic divisions to produce haploid spermatids (Schultz et al., 2003). Once meiosis is completed, spermatids condense their nucleus, eliminate residual components, develop the acrosome-acroplaxome complex and the manchette, and form the flagellum of the sperm tail (Kierszenbaum and Tres, 2004). Spermatids are then released from Sertoli cell apical crypts into the lumen of the seminiferous tubules and reach the epididymis to acquire forward motility.

The acrosome-acroplaxome complex is an essential structure during spermatid development needed for successful fertilization. The acrosome is a Golgi derived structure that stores hydrolytic enzymes released at fertilization upon completion of the acrosome reaction (Meizel, 1984). The acroplaxome is an F-actin-keratin cytoskeletal plate with a desmosome-like marginal ring anchoring the acrosome to the nucleus and modulating spermatid nuclear shaping (Buffone et al., 2012; Kierszenbaum et al., 2003). Caudally to the acrosome-acroplaxome is the manchette, a transient microtubule/F-actin-containing structure with a role in spermatid head shaping (Russell et al., 1991) in conjunction with the acrosome-acroplaxome complex. It is along the microtubules and F-actin tracts of the manchette that proteins are ferried by molecular motor proteins to the head-tail coupling apparatus (HTCA) and then along the flagellum through processes referred to as intramanchette transport (IMT) (Kierszenbaum, 2002) and intraflagellar transport (IFT) (Rosenbaum and Witman, 2002).

The flagellum is anchored to the head of the sperm through the HTCA, a centrosome-based structure that also contributes a basal body to initiate assembly of the microtubule axoneme of the flagellum (Irons, 1983; Rivkin et al., 2009). The importance of a functional HTCA to sperm development and male fertility is demonstrated by a truncating mutation in the rat hypodactylous (*hd*) locus that results in the expression of a truncated form of centrobin (*Cntrob*, for centrosome BRCA2 interacting protein, Zou et al., 2005). In *hd* mutant spermatids, there is a separation between the centrosome and its normal site of attachment to the nucleus. This separation results in the decapitation of the spermatid heads during final steps in the formation of spermatozoa. The decapitated tails became bundled in the lumen leading to an absence of functional sperm in the epididymis and to male infertility. This decapitation occurs due to a defective HTCA that is unable to stabilize the connection of the tail to the sperm nucleus (Liska et al., 2009). Similarly, decapitation and/or absence of flagellum assembly is also a common cause of infertility in mice and humans (Moretti et al., 2011; Mundy et al., 1995; Sauvalle et al., 1983; Wilton et al., 1992).

Despite the detailed knowledge about the sequence of events involved in spermatogenesis, our understanding of the process at the molecular level remains limited. Because the sperm flagellum is homologous to the motile cilia and flagella found on other eukaryotes, model systems such as *Tetrahymena thermophila* and *Chlamydomonas reinhardtii* have proven exceptionally useful in the discovery of genes linked to male infertility (Diniz et al., 2012). For example, the gene product for *MIA2* produces an axonemal dynein necessary for proper flagella movement in *C. reinhardtii* (Yamamoto et al., 2013). Mammals possess a potential homolog of the *MIA2* gene which is named *Coiled-coil domain containing 42* (*Ccdc42*) in mice, and whose function has yet to be reported. Other examples are *Ccdc39* and *Ccdc40,* both of which are necessary for the proper assembly and function of flagella and motile cilia in a variety of vertebrates and invertebrates (Blanchon et al., 2012; Merveille et al., 2011; Sui et al., 2015). We hypothesized that *Ccdc42* would have a similar role in motile cilia or flagella assembly and would thus be a candidate ciliopathy and infertility gene.

Here, we report our findings on mice with mutations in *Ccdc42*, a gene whose expression is greatly enriched in the testes at the onset of puberty and also in several regions in the brain. While we were unable to generate specific antisera to mammalian Ccdc42, utilizing *T. thermophila*, we demonstrate that the Ccdc42 homolog localizes to the base of motile cilia. Importantly, loss of *Ccdc42* in mice is associated with male infertility and an abnormal number and positioning of the HTCA and the mutant sperm lack an attached flagellum. While *Ccdc42* expression is also observed in the Purkinje cells of the cerebellum, *Ccdc42* null mutant mice did not display defects in coordinated motor activity or obvious behavioral abnormalities. In contrast to organisms with mutations in *Ccdc39* and *Ccdc40,* there were no overt defects observed in motile cilia in other tissues.

Materials and Methods

Generation of Ccdc42 Knockout Mice

The *Ccdc42* knockout allele (*Ccdc42*$^{tma(KOMP)Vlcg}$, Knockout Mouse Project Repository, Davis, CA USA; hereinafter referred to as *Ccdc42*^{KO}) was generated using embryonic stem cells in which all seven exons of the wild-type *Ccdc42* allele were removed and replaced with a β-galactosidase cassette. The correct targeting of the construct into *Ccdc42* was confirmed by genomic PCR and sequence analysis. PCR primers for genotyping were designed based on the insertion site (upstream: ACTAAAGCAGCCTCTAGCTG, lacZ: GTCTGTCCTAGCTTCCTCACTG, WT intron 1: GGTAAGGCAATTAGGAGCACTG). The knock-out allele generates a 313 bp band, while the wild-type allele generates a 392 bp band. The embryonic stem cells containing the targeted allele were derived from a C57BL/6N background and were injected into albino C57BL/6 blastocysts (C57BL/6J-*Tyrc-2J*; JAX Laboratories) by the UAB Transgenic Mouse Facility. Chimeras were then crossed with albino C57BL/6 females and germline transmission was confirmed by coat color of the offspring and subsequent PCR genotyping. All mice were maintained in accordance with IACUC regulations at the University of Alabama at Birmingham.

Ccdc42 Homolog Analysis

Homologs of Ccdc42 in other organisms was determined through analysis of the full length mouse polypeptide sequence of Ccdc42 using NCBI/BLAST (blast.ncbi.nlm.nih.gov/Blast.cgi). Coiled-coil domains present in Ccdc42 was determined using HMMER biosequence analysis (http://hmmer.janelia.org/) (Finn et al., 2011).

Reverse Transcription PCR Analysis

To assess *Ccdc42* expression, RNA was isolated using Trizol reagent according to the manufacturer's protocol (15596-026, Life Technologies, Carlsbad, CA USA). Once extracted, total RNA was used to synthesize cDNA using the Verso cDNA kit according to the manufacturer's protocol (AB-1453, Thermo Scientific, Pittsburgh, PA USA). PCR analysis was then performed using two sets of primers to determine expression of Ccdc42 (written 5' to 3'): ACTTGCGCTGGGAAGAACTA and CTTGCAGCTTGACACTCAGC which span intron 3 and 4, in some experiments the primers GGACTCGAGACCATGAGTTTGGGCATGGAA and GTACCCGGGACATCCGGACTTGCTGTTG were used which flank the sequence between the first and last exons of the $Ccdc42^{WT}$ allele. Both sets of primers yielded identical results. Control actin primers were used in all samples: ATGGGTCAGAAGGACTCCTA and GGTGTAAAACGCAGCTCA. All results were confirmed in at least three animals.

β-Galactosidase Assays

Organs were dissected from $Ccdc42^{WT}$, $Ccdc42^{Het}$, and $Ccdc42^{KO}$ mice at 8 weeks of age. Organs were fixed overnight at 4°C in 4% PFA in PBS and subsequently washed in PBS. Tissues were then cryoprotected with 30% sucrose in PBS for 24 hours, and snap frozen in OCT freezing compound (Tissue-Tek, Torrance, CA USA). 10 μm thick cryosections were cut with a Leica CM1900 cryostat mounted on slides and postfixed in 4% PFA in PBS for 10 minutes, washed three times with LacZ wash buffer (2 mM $MgCl_2$, 0.01% sodium deoxycholate, 0.02% NP-40, in 100 mM sodium phosphate buffer, pH 7.3), and then incubated in X-gal staining solution (2 mM $MgCl_2$, 5 mM potassium ferrocyanide, 5 mM potassium ferricyanide, 1 mg/ml X-Gal, in PBS) at 37°C overnight. Sections were then counterstained in Fast Red for 5 minutes, dehydrated using an ethanol and xylene series and cover slipped with Permount mounting media (Fisher Scientific, Pittsburg, PA USA). Images were captured on a Nikon TE2000s microscope (Nikon instriments inc., Melville, NY) equipped with a Micropublisher 3.3 CCD camera (Qimaging, Surrey, BC, Canada) using Qcapture Pro 5.1.

Testing Fertility of $Ccdc42^{KO}$ Mice

To determine if $Ccdc42^{KO}$ mice were capable of producing offspring, a $Ccdc42^{KO}$ mouse was paired with a wild-type ($Ccdc42^{WT}$) mouse of the opposite sex. Copulation was determined by the presence of a vaginal mucous plug the next day, after which the female was isolated and observed to determine the number of pups born. Fertility was considered as a measurement of the average litter size. Statistically significant differences in litter size were determined by Kruskal-Wallis one way ANOVA followed by Dunn's post-hoc test.

Histology

Testes were dissected from *Ccdc42*^{WT} and *Ccdc42*^{KO} mice, cut in half, and fixed with Bouin's fixative solution (1120–16, Ricca Chemical Company, Arlington, TX USA) for 24 hours. Tissue was then rinsed thoroughly in tap water, dehydrated, embedded in paraffin, and cut into 10 μm sections following standard procedures. Sections were stained with periodic acid-Schiff (PAS) stain and counterstained with hematoxylin. Sections were imaged as described above. In addition, 1μm-thick sections of epoxy-embedded testis and epididymis *Ccdc42*^{WT} and *Ccdc42*^{KO} mice, fixed sequentially in glutaraldehyde and osmium tetroxide according to a standard procedure (see below), were stained with 1% toluidine blue (Kierszenbaum et al., 2003) and examined using a Zeiss microscope (Thornwood, NY) equipped with an Optronics Magnafire (Goleta, CA) digital camera.

Transmission electron microscopy of mouse testes

Testes and epididymides from *Ccdc42*^{WT} and *Ccdc42*^{KO} mice were fixed in 2.5% glutaraldehyde in 0.1M phosphate buffer (pH 6.9), then postfixed in 2% osmium tetroxide in the same buffer and embedded in a plastic resin. Thin sections were stained with 5% uranyl acetate in methanol followed by lead citrate and examined using a JEM-100CX transmission electron microscope (JEOL Ltd., Japan) operated at an accelerating voltage of 60 kV.

Coordination testing of mice

Mice were placed on a Rotor-Rod apparatus (San Diego Instruments Inc, San Diego, CA) starting at a speed of 4rpm. After 10 seconds the rod was accelerated at a constant rate up to 50rpm over 140 seconds. Fall time was recorded electronically by an infrared beam. Animals were removed from the apparatus and returned to their home cage for 15 minutes between each trial. Each mouse was tested 3 times. Latency to fall and total distance run was recorded for each trial. Statistically significant differences in fall latency were assessed by Student's t-test.

Generation of GFP-Ccdc42 Tetrahymena thermophila

To express GFP-tagged Ccdc42 in *Tetrahymena thermophila* cells, the coding region of the putative *T. thermophila Ccdc42* homolog (TTHERM_00730320) was cloned into pMTT1-GFP to generate pMTT1-GFP-Ccdc42. The DNA was amplified with primers carrying MluI (5'-TATATACGCGTCATGATTAATAAAATAAAATCTAAT-3') and BamHI (5'-TAATTGGATCCCTATCAATAGTTGTATTTAGTTTATTT-3') sites. The transgene was introduced into starved CU522 *Tetrahymena thermophila* cells with a Bio-Rad Model PDS-1000/He Biolistic Particle Delivery System. Briefly, *T. Thermophila* were bombarded with SacII- and XhoI-digested pMTT1-GFP-Ccdc42 plasmid and transformants were selected from SPP medium (1% proteose peptone, 0.2% glucose, 0.1% yeast extract, and 0.003% EDTA ferric sodium salt) with 20 μM paclitaxel. Using this approach, the transgene integrated by homologous recombination into the nonessential *BTU1* gene which carries a mutation conferring sensitivity to paclitaxel(Shang et al., 2002). The copy number of the transgene was increased by allowing cells to sort the mutant *BTU1* allele during vegetative propagation in the presence of paclitaxel. To induce expression of GFP-Ccdc42, cells were incubated in 2.5 μg/ml $CdCl_2$ (202908, Sigma-Aldrich, St. Louis, MO) for 2 hours.

Immunofluorescence of Tetrahymena thermophila

GFP-Ccdc42 *Tetrahymena* cells were isolated onto coverslips and were fixed and permeabilized with 2% paraformaldehyde and 0.5% Triton X-100 in PBS buffer. Cells were then air dried at 30°C and blocked with 1% BSA in PBS for 1 hour. Immunofluorescence with 12G10 anti-α-tubulin monoclonal antibody (1:10, Developmental Studies Hybridoma Bank, University of Iowa) and 2302 anti-polyglycylation polyclonal antibody (1:300, generously provided by Martin A. Gorovsky) was performed by incubating cells in primary antibody diluted in 1% BSA in PBS overnight at 4°C. Cells were then washed with PBS and incubated in secondary antibodies for one hour at room temperature. Secondary antibodies included Alexa Fluor-647 and 594 conjugated donkey anti-rabbit and anti-mouse (Invitrogen, Carlsbad, CA USA). Nuclei were visualized by Hoechst nuclear stain (Invitrogen, Carlsbad, CA USA). Stained cells were mounted using DABCO mounting media (10 mg of DABCO (Sigma-Aldrich, St. Louis, MO USA) in 1 mL of PBS and 9 mL of glycerol).

Results

Amino acid sequence of Ccdc42 and its primary structure

To assess the level of conservation of Ccdc42, we compared protein sequences of the Ccdc42 homologs in mice, humans, Tetrahymena thermophila, and Chlamydomonas reinhardtii using NCBI/BLAST (blast.ncbi.nlm.nih.gov/Blast.cgi) (Fig. 1A). Both human and mouse proteins have a calculated mass of approximately 38 kDa, are 316 amino acids in length, and have an 86 pairwise score (86% identity). The Ccdc42 homolog in *C. reinhardtii*, named FAP73 (protein product of *MIA2*) is necessary for proper flagella mediated cell motility, and has an approximate 25 pairwise score with the mouse Ccdc42 protein (Yamamoto et al., 2013). Sequence analysis determined the protein product of the *T. thermophila* gene TTHERM_00730320 has a pairwise score of 22 with mouse Ccdc42, but no studies on this gene or protein product in *T. thernmophila* have been previously reported. Notably, another annotation of the *T. thermophila* genome lists a start codon 177 bases downstream of the start codon for TTHERM_00730320, shifting the reading frame and generating an alternate gene, named TTHERM_000730311 that has minimal homology with Ccdc42. Potentially, this is indicative that the two are overlapping genes, but further research is necessarily to clarify this possibility. Ccdc42 is named after the coiled-coil domains found in the protein structure, which are present in all four listed homologs (Coiled-coil domains were found using HMMER(Finn et al., 2011)). Additionally, portions of the coiled-coil domains overlap in mouse, human, *T. thermophila*, and *C. reinhardtii* (Fig. 1). This suggests the coiled-coil domains may be important for function of the Ccdc42 protein.

Ccdc42^{KO} mice are viable

To determine the function of Ccdc42 in a mammalian system, a knockout mouse line was established using a null allele that resulted in loss of all seven exons of the wild-type *Ccdc42* allele and replaced it with a lacZ reporter and neomycin resistance cassette (Fig. 1B). *Ccdc42* heterozygotes were crossed to one another to produce wild-type (*Ccdc42*^{WT}), *Ccdc42* heterozygous (*Ccdc42*^{Het}), and *Ccdc42* homozygous knockout mice (*Ccdc42*^{KO}), which were differentiated through genomic DNA PCR genotyping (Fig. 1D). *Ccdc42*^{KO}

mice are born at a rate that did not significantly deviate from the Mendelian ratio (69 WT, 132 Het, 66 Mut, $\chi^2 = 0.101$, P = 0.95) and showed no obvious physical signs of improper development or ill-health (Fig. 1C).

Testes express Ccdc42 in an age- and cell-dependent manner

Survival of *Ccdc42*^{KO} mice indicates that Ccdc42 is dispensable to proper development. To better understand what potential biological processes were being disrupted in *Ccdc42*^{KO} mice, we conducted RT-PCR analysis on tissue harvested from adult mice (8 weeks of age) to determine where *Ccdc42* is expressed. We found that *Ccdc42* is predominantly expressed in the testes and also in the brain (Fig. 2A). *Ccdc42* expression in the testes appears in a developmentally-dependent manner. *Ccdc42* expression in the testes is initiated at approximately ten days of age and is maintained into adulthood (Fig. 2A, B). This time course corresponds with the onset of meiosis, providing evidence for a role for Ccdc42 in sperm production. In contrast, no expression of *Ccdc42* was observed in ovaries harvested from 8-week-old female mice.

We used the β-galactosidase (β-gal) reporter cassette incorporated into the mutant allele to determine which cells in the brain and testes express *Ccdc42*. Strong β-galactosidase activity was observed in the spermatids within the lumen of the seminiferous tubules in testes from 8-week-old *Ccdc42*^{Het} mice (Fig. 2C), while cells adjacent to the basement membrane of the tubule, including Sertoli cells, spermatogonia and spermatocytes (identified by morphology and histology) did not display β-galactosidase activity. The testosterone-producing Leydig cells, scattered in-between the seminiferous tubules, also lacked β-galactosidase activity. This pattern of staining indicates that *Ccdc42* expression in the testes appears limited to adluminal spermatids that are engaged in the assembly of flagella.

β-galactosidase activity was clearly observed in the Purkinje cells of the cerebellum (Fig. 2C) with very slight staining in the pyramidal layer of the hippocampus, the striatum, and amygdala and speckled throughout the cerebral cortex (Supp. Fig. 1). Since the Purkinje cells are involved in coordinating motor activity and cilia are important for normal cerebellar development, we tested the *Ccdc42*^{KO} mice for any muscle coordination defects using the rotarod behavioral test(Chizhikov et al., 2007). No significant difference were observed between the performance of the *Ccdc42*^{KO} mice and their wild-type littermates (latency to fall: 54.5±13.9s vs. 45.7±5.1s, p=0.54, Student's t-test), indicating Ccdc42 is not necessary for proper muscle coordination.

Male Ccdc42^{KO} mice are sterile

Given the expression of *Ccdc42* in the testes, we assessed whether the *Ccdc42*^{KO} mice display reduced fertility. *Ccdc42*^{KO} males were able to mate with females, as evidenced by the presence of a vaginal mucous plug the morning after a mating pair was established, however, no offspring were ever produced from these pairings (Table 1.). When crossed with *Ccdc42*^{WT} males, *Ccdc42*^{KO} females produced litters at a frequency and of a size that did not significantly deviate from control *Ccdc42*^{WT} male by *Ccdc42*^{WT} female matings.

Structural characteristics of the testes and epididymides of Ccdc42^{WT} and Ccdc42^{KO} mice

As we observed β-galactosidase reporter activity in the developing spermatids of *Ccdc42^{Het}* and *Ccdc42^{KO}* males, we next examined spermatid development in *Ccdc42^{KO}* males to determine if infertility was a result of improper spermatid structure. A histologic screening of testes and epididymides revealed that the seminiferous tubules of *Ccdc42^{WT}* displayed a lumen with flagella projecting from developing spermatids with periodic acid Schiff-stained acrosomes (Fig. 3A). In contrast, the seminiferous tubules of *Ccdc42^{KO}* mice lacked flagella projecting into a well-defined lumen (Fig. 3B). At high magnification, the seminiferous epithelium of *Ccdc42^{WT}* mice shows structurally normal spermatogenic cells, including flagellated mature spermatids being released into the seminiferous tubular lumen during spermiation (Fig. 3C). *Ccdc42^{KO}* testes have elongating spermatids with abnormally shaped heads coexisting with structurally unaffected spermatogenic cells populating the adjacent region of seminiferous epithelium (Fig. 3D). The lumen of the epididymal duct of *Ccdc42^{WT}* mice is filled with abundant flagellated sperm (Fig. 3E) but there is a complete lack of sperm in the epididymal lumen of *Ccdc42^{KO}* mice, which instead contain only cellular debris (Fig. 3F). These observations indicate that the structural defects of spermiogenesis in *Ccdc42^{KO}* mice, including irregular spermatid head shaping, coincide with a failure of spermiation and degradation of maturing spermatids within the testis.

Morphological abnormalities of Ccdc42^{KO} sperm cells

We used transmission electron microscopy to understand the mechanism underlying the defect in flagella assembly in the spermatids of *Ccdc42^{KO}* mice. We focused on the HTCA (also known as the connecting piece), which is the site of origin of the axoneme and also a critical structure involved in sperm head-tail joining. Spermatids of wild-type mice have a centrosome consisting of a proximal centriole closely associated with the implantation fossa of the spermatid nucleus and a distal centriole engaged in the development of the axoneme (Fig. 4A). A banded collar encircles the centriolar complex. Three significant alterations are observed in spermatids of *Ccdc42^{KO}* mice: there is often a multiplicity of HTCAs (three HTCAs are shown in Fig. 4B, indicated with arrows), aberrant in-folding of the acrosome-acroplaxome complex leading to abnormal nuclear shaping (Fig. 4D), and the dislocation of the HTCA from its native implantation site (Fig. 4C). A consistent structural feature is the presence of multiple vesicles at the HTCA developmental sites (one of the three HTCA shown in Fig. 4B and a single HTCA seen in Fig. 4C), some of them containing dense material of unknown nature. Although microtubular manchettes are observed in elongating spermatids (Fig. 4B–D), no assembly of axonemal microtubules emerge from the HTCA as is seen in the equivalent wild-type spermatids (see Fig. 4A, label number 6). In what appears to be a mature degenerating *Ccdc42^{KO}* spermatid we observe that the nuclear envelope surrounding the condensed nucleus has begun to rupture along with an abortive and detached acrosome-acroplaxome complex (Fig. 4E). The mitochondria, which under normal conditions would migrate to encircle the middle segment of the axoneme, have clustered around the nucleus, while a pair of HTCAs, still lacking axonemes, remains anchored to a fragment of condensed nuclear material. Even though a microtubular manchette is available for intramanchette transport of cargo toward the HTCA and the developing axoneme and associated outer dense fibers and fibrous sheath are all present in the *Ccdc42^{KO}* spermatids,

the HTCAs do not seem to be initiating flagellogenesis, concurrent with defective nuclear shaping and abortive acrosome development in mature spermatids.

Tetrahymena thermophila have a putative homolog of Ccdc42 that localizes to the base of the cilia

Assessing the function of a gene and its protein product in sperm cells can be difficult. By their nature, sperm are short-lived and non-dividing cells, making them difficult to maintain in culture. The highly condensed nature of the sperm nucleus renders the cell essentially transcriptionally silent which makes the expression of fluorescently tagged proteins nearly impossible. Multiple attempts to generate Ccdc42 specific antisera and the use of commercial Ccdc42 antibodies were unsuccessful using both western blot and by immunofluorescence approaches, as were attempts to localize the protein by transfecting GFP tagged Ccdc42 into cultured cell lines and testes explants (Supp. Fig. 2). Therefore, we sought other organisms with homologs of *Ccdc42* where gene function could be assessed at the cellular level. Interestingly, organisms with only primary cilia (e.g. *C. elegans*) do not possess putative *Ccdc42* homologs, but most organisms with motile cilia (e.g. *C. reinhardtii*, *T. thermophile*, mice, and humans) do have a homolog. Using NCBI/BLAST (blast.ncbi.nlm.nih.gov/Blast.cgi), we found a putative homolog of *Ccdc42* in *T. thermophila* designated TTHERM_00730320 (which will hereafter be referred to as *Ccdc42*). To determine the localization of Ccdc42 in *T. thermophila*, we cloned *Ccdc42* into the pMTT1-GFP plasmid, which expresses a gene of interest tagged with GFP in response to the presence of cadmium chloride ($CdCl_2$). In the uninduced state ($-CdCl_2$), no GFP signal was detected, but two hours after $CdCl_2$ administration, robust expression of GFP was observed. Co-staining the induced GFP-Ccdc42 *T. thermophila* with an antibody against α-tubulin (12G10) to label cilia tips and an antibody against polyglycylated tubulin (2302) to label the axoneme of cilia, revealed that GFP localizes specifically to the base of each motile cilium (Fig. 5B). This localization would be consistent with a role in basal bodies similar to the HTCA in sperm.

Discussion

Our studies of *Ccdc42* reveal a gene whose expression pattern in testes coincides with onset of puberty and sperm development, the loss of which is associated with male infertility. Despite some expression of *Ccdc42* in the brain, the $Ccdc42^{KO}$ mice display no obvious signs of abnormal development, motor activity, or behavior. The $Ccdc42^{KO}$ mutants were visually indistinguishable from wild-type siblings. Furthermore, the entire coding sequence of *Ccdc42* is deleted from our $Ccdc42^{KO}$ allele, making it unlikely that alternate transcripts might mask other phenotypes. One possibility is that expression of a related gene, *Ccdc42b*, is compensating for loss of *Ccdc42* expression in certain cell types of the mouse. Furthermore, the possibility remains that the observed mutant phenotypes could be due to perturbing regulatory elements of genes located near *Ccdc42*. However, current genome annotations do not list any other genes overlapping *Ccdc42*. Additionally, the localization of the Ccdc42 homolog to the base of the motile cilia in *T. thermophila*, and the defect in flagella motility observed in mutant *C. reinhardtii* suggests that our observations in male $Ccdc42^{KO}$ mice are due to loss of functional *Ccdc42*.

The observation that *Ccdc42* expression was upregulated in the testes between 10 – 15 days of age is informative, as previous reports found that at approximately 12 days of age the expression of many genes necessary for sperm development and flagella assembly is significantly increased (Horowitz et al., 2005). Male mice are not capable of producing mature sperm cells until approximately 35 days of age and it is believed that the increased expression of genes allows the first wave of morphological changes (including nuclear condensation and flagellum assembly) necessary to create mature sperm (Leblond and Clermont, 1952). Before 12 days of age, spermatogenic cells within the testes are generally undergoing mitotic cell divisions, initiate meiosis and are not yet engaged in spermiogenesis involved in building a flagellum or undergoing nuclear condensation. The fact that *Ccdc42* is not expressed before 10–15 days of age indicates that the gene is dispensable for these early cell divisions, and instead suggests a role with the morphogenesis of the cells into mature sperm. In fact, the β-galactosidase activity staining assays for *Ccdc42* expression show that Sertoli cells, Leydig cells, spermatogonia, and spermatocytes do not express significant levels of *Ccdc42.* The appearance of staining in spermatids argues in favor of a specialized function of the gene in spermiogenesis during formation of the flagellum.

Also of importance is the fact that $Ccdc42^{KO}$ males still produced copulatory plugs and were mating with females, thus confirming that the sterility phenotype was not due to reproductive behavior abnormalities. $Ccdc42^{KO}$ females had normal fertility, consistent with the fact that expression was found in the testes, but not in the ovaries or oviducts. As motile cilia are needed to move embryos to the uterus, the normal fertility of $Ccdc42^{KO}$ females indirectly supports the notion that *Ccdc42* is not necessarily for motile cilia assembly or function.

One of the causes of sperm decapitation and abnormal tail development is the disruption of the delivery of cargo to specific assembly sites by intramanchette transport and intraflagellar transport(Kierszenbaum et al., 2011). A previous study of *hd* mutant rats expressing truncated *Cntrob*, a coiled-coil protein similar to Ccdc42, displayed spermatid/sperm decapitation at the HTCA (Liska et al., 2009). *Cntrob* generates the protein centrobin, which is a daughter centriole protein essential for centrosome duplication and elongation, two functions depending on centrobin-tubulin interaction (Gudi et al., 2011). However, the $Ccdc42^{KO}$ sperm with multiple HTCAs and no axoneme differ from the decapitated sperm of the *hd* mutant rats that have a single HTCA and a developed axoneme. $Ccdc42^{KO}$ spermatids often display detached and degraded acrosomes, in addition to abnormalities in nuclear folding. *hd* and $Ccdc42^{KO}$ mutants display head shaping abnormalities, suggesting that both the expression of truncated *Cntrob* and a lack of *Ccdc42* expression impact the normal function of the acrosome-acroplaxome-manchette complex. Nevertheless, other mutant mice with acrosome and nuclear shaping defects are often still able to assemble flagella, such as in the acrosome-deficient Hrb mutant mice (Kierszenbaum and Tres, 2004). In contrast, $Ccdc42^{KO}$ sperm demonstrate defects not only in the acrosome-acroplaxome, but also the HTCA and flagellum.

Cargo transport along the transiently formed manchette is essential for spermiogenesis and may not only require the developmental timed function of microtubule- and F-actin-based molecular motors and intraflagellar proteins such as IFT88, but also the stabilizing role of

coiled-coil proteins, including Ccdc42 and centrobin among others. In this scenario, loss of *Ccdc42* expression could prevent the transport of proteins leading to defects in the HTCA and subsequent inability to build a flagellum, in addition to contributing to the mispositioning of the mitochondria. Alternatively, Ccdc42 may be a passenger protein transported along the manchette from the acrosome-acroplaxome complex to the HTCA where it may then determine the proper number, placement and stability of the HTCA. Oddly, *C. reinhardtii* mutant for the putative Ccdc42 homolog, FAP73 (protein product of *MIA2*), only display defects in flagella beating, while $Ccdc42^{KO}$ spermatozoa are completely lacking in flagella altogether (Yamamoto et al., 2013). FAP73 is located within the flagella axoneme and thought to be a regulator of inner and outer dynein arm activity. These differences could indicate evolutionary divergence in function between the two genes.

The extra number of centrosome-based HTCAs in $Ccdc42^{KO}$ sperm raises the possibility that centrosomes are being asymmetrically partitioned after meiosis or that the mechanism that ensures a single centrosome in developing haploid spermatids is faulty. Mouse spermatids developed *in vitro* from pre-existing spermatocytes can display up to four motile axonemes (Marh et al., 2003), each presumably derived from an independent basal body. During meiosis, the centrosomes duplicate and are sorted into what will become the two new daughter cells. Given the fact that some $Ccdc42^{KO}$ sperm cells contain a loss of the HTCA while others contain an excess, it remains possible that Ccdc42 is necessary for the sorting of the centrosomes in spermatozoa cell division. The abnormal number of HTCA structures might also indicate that loss of Ccdc42 causes abnormal degradation and *de novo* assembly of new centrosomes, also leading to disruption of flagella assembly.

The infertility phenotype in male $Ccdc42^{KO}$ mice in the absence of other maladies raises the possibility that homozygous loss of function mutations in *CCDC42* are a cause of male infertility in human patients with no additional overt phenotypes. As female $Ccdc42^{KO}$ mice show no defects in fertility, such a deleterious allele would have a higher chance of being passed onto future generations compared to those that affect both male and female fertility. Similar findings have been documented with other mutant mice. For example, *azh* mutant mice also have a male infertility phenotype due to abnormal sperm head shaping (Meistrich et al., 1990; Mochida et al., 1999). The *azh* mutant mice were later found to harbor mutations in the gene *Hook1*, whose protein product localizes to the acrosome-acroplaxome complex and manchette in a similar fashion to Ccdc42 (Mendoza-Lujambio et al., 2002). However, unlike $Ccdc42^{KO}$, the *azh* mutant spermatids are still able to assemble flagella, indicating distinct differences in molecular function. Future studies screening male infertility patients for mutations in *CCDC42* will help to address this question and provide more insights into its molecular function.

Supplementary Material

Refer to Web version on PubMed Central for supplementary material.

Acknowledgments

This work was supported in part by RO1 DK065655 (BKY) and P30 DK074038 (BKY), T32 graduate training award (T32 GM008111, BKY) to RCP and F32 postdoctoral awards (F32 DK088404) to NFB. The UAB

Transgenic Mouse Facility and RAK are supported by NIH P30 CA13148, P30 AR048311 and P30 DK074038. We would like to thank Mandy J. Croyle and Devan Rockwell for technical assistance and Dr. Michael A. Miller (UAB) for generously allowing us use of his Bio-Rad Model PDS-1000/He Biolistic Particle Delivery System.

References

Blanchon S, Legendre M, Copin B, Duquesnoy P, Montantin G, Kott E, Dastot F, Jeanson L, Cachanado M, Rousseau A, Papon JF, Beydon N, Brouard J, Crestani B, Deschildre A, Desir J, Dollfus H, Leheup B, Tamalet A, Thumerelle C, Vojtek AM, Escalier D, Coste A, de Blic J, Clement A, Escudier E, Amselem S. Delineation of CCDC39/CCDC40 mutation spectrum and associated phenotypes in primary ciliary dyskinesia. J Med Genet. 2012; 49:410–416. [PubMed: 22693285]

Borg CL, Wolski KM, Gibbs GM, O'Bryan MK. Phenotyping male infertility in the mouse: how to get the most out of a 'non-performer'. Human reproduction update. 2010; 16:205–224. [PubMed: 19758979]

Buffone MG, Ijiri TW, Cao W, Merdiushev T, Aghajanian HK, Gerton GL. Heads or tails? Structural events and molecular mechanisms that promote mammalian sperm acrosomal exocytosis and motility. Molecular reproduction and development. 2012; 79:4–18. [PubMed: 22031228]

Chizhikov VV, Davenport J, Zhang Q, Shih EK, Cabello OA, Fuchs JL, Yoder BK, Millen KJ. Cilia proteins control cerebellar morphogenesis by promoting expansion of the granule progenitor pool. The Journal of neuroscience : the official journal of the Society for Neuroscience. 2007; 27:9780–9789. [PubMed: 17804638]

De Kretser DM, Baker HW. Infertility in men: recent advances and continuing controversies. The Journal of clinical endocrinology and metabolism. 1999; 84:3443–3450. [PubMed: 10522977]

Diniz MC, Pacheco AC, Farias KM, de Oliveira DM. The Eukaryotic Flagellum Makes the Day: Novel and Unforeseen Roles Uncovered After Post-Genomics and Proteomics Data. Current protein & peptide science. 2012

Finn RD, Clements J, Eddy SR. HMMER web server: interactive sequence similarity searching. Nucleic acids research. 2011; 39:W29–37. [PubMed: 21593126]

Gudi R, Zou C, Li J, Gao Q. Centrobin-tubulin interaction is required for centriole elongation and stability. The Journal of cell biology. 2011; 193:711–725. [PubMed: 21576394]

Holden CA, McLachlan RI, Pitts M, Cumming R, Wittert G, Agius PA, Handelsman DJ, de Kretser DM. Men in Australia Telephone Survey (MATeS): a national survey of the reproductive health and concerns of middle-aged and older Australian men. Lancet. 2005; 366:218–224. [PubMed: 16023512]

Horowitz E, Zhang Z, Jones BH, Moss SB, Ho C, Wood JR, Wang X, Sammel MD, Strauss JF 3rd. Patterns of expression of sperm flagellar genes: early expression of genes encoding axonemal proteins during the spermatogenic cycle and shared features of promoters of genes encoding central apparatus proteins. Mol Hum Reprod. 2005; 11:307–317. [PubMed: 15829580]

Irons MJ. Synthesis and assembly of connecting-piece proteins as revealed by radioautography. Journal of ultrastructure research. 1983; 82:27–34. [PubMed: 6848771]

Kierszenbaum AL. Intramanchette transport (IMT): managing the making of the spermatid head, centrosome, and tail. Molecular reproduction and development. 2002; 63:1–4. [PubMed: 12211054]

Kierszenbaum AL, Rivkin E, Tres LL. Acroplaxome, an F-actin-keratin-containing plate, anchors the acrosome to the nucleus during shaping of the spermatid head. Molecular biology of the cell. 2003; 14:4628–4640. [PubMed: 14551252]

Kierszenbaum AL, Rivkin E, Tres LL. Cytoskeletal track selection during cargo transport in spermatids is relevant to male fertility. Spermatogenesis. 2011; 1:221–230. [PubMed: 22319670]

Kierszenbaum AL, Tres LL. The acrosome-acroplaxome-manchette complex and the shaping of the spermatid head. Archives of histology and cytology. 2004; 67:271–284. [PubMed: 15700535]

Leblond CP, Clermont Y. Spermiogenesis of rat, mouse, hamster and guinea pig as revealed by the periodic acid-fuchsin sulfurous acid technique. The American journal of anatomy. 1952; 90:167–215. [PubMed: 14923625]

Liska F, Gosele C, Rivkin E, Tres L, Cardoso MC, Domaing P, Krejci E, Snajdr P, Lee-Kirsch MA, de Rooij DG, Kren V, Krenova D, Kierszenbaum AL, Hubner N. Rat hd mutation reveals an essential role of centrobin in spermatid head shaping and assembly of the head-tail coupling apparatus. Biology of reproduction. 2009; 81:1196–1205. [PubMed: 19710508]

Marh J, Tres LL, Yamazaki Y, Yanagimachi R, Kierszenbaum AL. Mouse round spermatids developed in vitro from preexisting spermatocytes can produce normal offspring by nuclear injection into in vivo-developed mature oocytes. Biology of reproduction. 2003; 69:169–176. [PubMed: 12620938]

Meistrich ML, Trostle-Weige PK, Russell LD. Abnormal manchette development in spermatids of azh/azh mutant mice. The American journal of anatomy. 1990; 188:74–86. [PubMed: 2346121]

Meizel S. The importance of hydrolytic enzymes to an exocytotic event, the mammalian sperm acrosome reaction. Biological reviews of the Cambridge Philosophical Society. 1984; 59:125–157. [PubMed: 6231059]

Mendoza-Lujambio I, Burfeind P, Dixkens C, Meinhardt A, Hoyer-Fender S, Engel W, Neesen J. The Hook1 gene is non-functional in the abnormal spermatozoon head shape (azh) mutant mouse. Hum Mol Genet. 2002; 11:1647–1658. [PubMed: 12075009]

Merveille AC, Davis EE, Becker-Heck A, Legendre M, Amirav I, Bataille G, Belmont J, Beydon N, Billen F, Clement A, Clercx C, Coste A, Crosbie R, de Blic J, Deleuze S, Duquesnoy P, Escalier D, Escudier E, Fliegauf M, Horvath J, Hill K, Jorissen M, Just J, Kispert A, Lathrop M, Loges NT, Marthin JK, Momozawa Y, Montantin G, Nielsen KG, Olbrich H, Papon JF, Rayet I, Roger G, Schmidts M, Tenreiro H, Towbin JA, Zelenika D, Zentgraf H, Georges M, Lequarre AS, Katsanis N, Omran H, Amselem S. CCDC39 is required for assembly of inner dynein arms and the dynein regulatory complex and for normal ciliary motility in humans and dogs. Nat Genet. 2011; 43:72–78. [PubMed: 21131972]

Mochida K, Tres LL, Kierszenbaum AL. Structural and biochemical features of fractionated spermatid manchettes and sperm axonemes of the azh/azh mutant mouse. Molecular reproduction and development. 1999; 52:434–444. [PubMed: 10092124]

Moretti E, Geminiani M, Terzuoli G, Renieri T, Pascarelli N, Collodel G. Two cases of sperm immotility: a mosaic of flagellar alterations related to dysplasia of the fibrous sheath and abnormalities of head-neck attachment. Fertility and sterility. 2011; 95:1787 e1719–1723. [PubMed: 21144504]

Mundy AJ, Ryder TA, Edmonds DK. Asthenozoospermia and the human sperm mid-piece. Hum Reprod. 1995; 10:116–119. [PubMed: 7745038]

Rivkin E, Kierszenbaum AL, Gil M, Tres LL. Rnf19a, a ubiquitin protein ligase, and Psmc3, a component of the 26S proteasome, tether to the acrosome membranes and the head-tail coupling apparatus during rat spermatid development. Developmental dynamics : an official publication of the American Association of Anatomists. 2009; 238:1851–1861. [PubMed: 19517565]

Rosenbaum JL, Witman GB. Intraflagellar transport. Nature reviews Molecular cell biology. 2002; 3:813–825. [PubMed: 12415299]

Russell LD, Russell JA, MacGregor GR, Meistrich ML. Linkage of manchette microtubules to the nuclear envelope and observations of the role of the manchette in nuclear shaping during spermiogenesis in rodents. The American journal of anatomy. 1991; 192:97–120. [PubMed: 1759685]

Sauvalle A, Le Bris C, Izard J. Supernumerary microtubules and prolongation of the middle piece in two infertile patients. International journal of fertility. 1983; 28:173–176. [PubMed: 6140238]

Schultz N, Hamra FK, Garbers DL. A multitude of genes expressed solely in meiotic or postmeiotic spermatogenic cells offers a myriad of contraceptive targets. Proceedings of the National Academy of Sciences of the United States of America. 2003; 100:12201–12206. [PubMed: 14526100]

Shang Y, Song X, Bowen J, Corstanje R, Gao Y, Gaertig J, Gorovsky MA. A robust inducible-repressible promoter greatly facilitates gene knockouts, conditional expression, and overexpression of homologous and heterologous genes in Tetrahymena thermophila. Proceedings of the National Academy of Sciences of the United States of America. 2002; 99:3734–3739. [PubMed: 11891286]

Sui W, Hou X, Che W, Ou M, Sun G, Huang S, Liu F, Chen P, Wei X, Dai Y. CCDC40 mutation as a cause of primary ciliary dyskinesia: a case report and review of literature. Clin Respir J. 2015

Wilton LJ, Temple–Smith PD, de Kretser DM. Quantitative ultrastructural analysis of sperm tails reveals flagellar defects associated with persistent asthenozoospermia. Hum Reprod. 1992; 7:510–516. [PubMed: 1522195]

Yamamoto R, Song K, Yanagisawa HA, Fox L, Yagi T, Wirschell M, Hirono M, Kamiya R, Nicastro D, Sale WS. The MIA complex is a conserved and novel dynein regulator essential for normal ciliary motility. The Journal of cell biology. 2013; 201:263–278. [PubMed: 23569216]

Highlights

- *Ccdc42* is expressed in the testes at the onset of puberty and in the brain
- *Ccdc42* is required for spermatogenesis
- *Ccdc42* mutations cause sperm decapitation and disrupts sperm motility

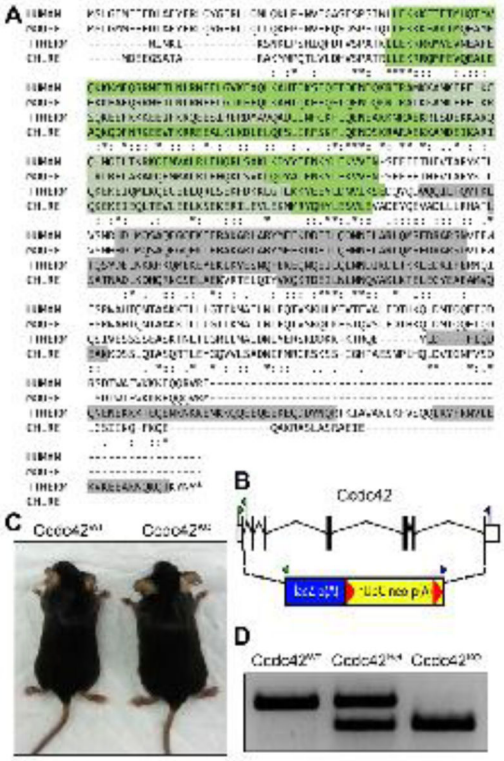

Figure 1. Ccdc42 homologs and generation of a knockout mouse allele

(A) ClustalW protein alignment of the human, mouse, *Tetrahymena thermophila*, and *Chlamydomonas reinhardtii* Ccdc42 homologs. Below the alignment (*) indicates identical, (:) conserved, and (.) semi-conservative amino acids. Gray highlight indicates coiled-coil motif. Green highlight indicates DUF4200 domains. (B) The Ccdc42 knockout allele was generated by replacing all 7 exons with a lacZ-p(A) reporter cassette (blue box). Location of primers used for genotyping are indicated by the blue and green triangles. (C) Wild-type control (*Ccdc42*^{WT}) mouse next to a knockout (*Ccdc42*^{KO}) sibling show no overt phenotypes in the mutants. (D) Genomic DNA PCR genotyping of wild-type (*Ccdc42*^{WT}), heterozygous (*Ccdc42*^{Het}) and knockout (*Ccdc42*^{KO}) mice.

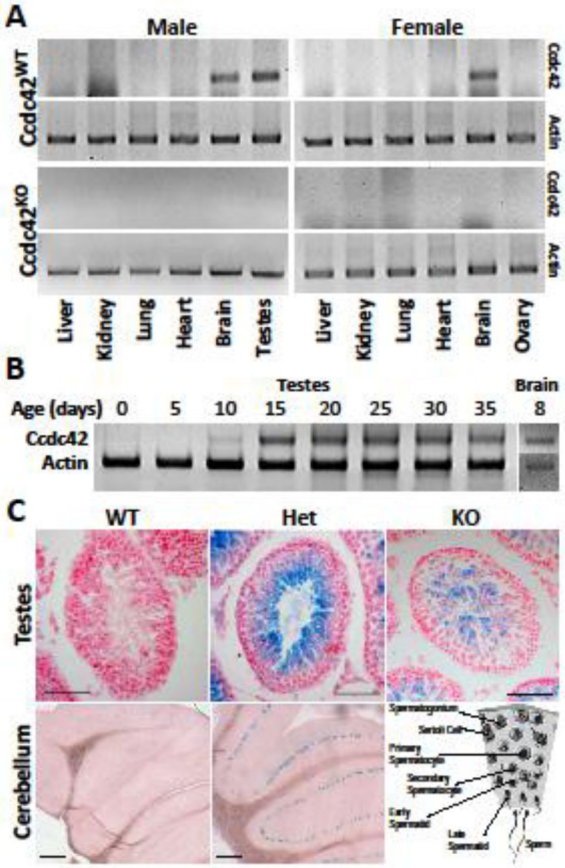

Figure 2. Ccdc42 expression in the mouse

(A) RT-PCR for *Ccdc42* in several tissues derived from 8-week old mice. Expression is limited to testes and brain. (B) RT-PCR analysis for *Ccdc42* in the developing testes. Expression begins at approximately 10 days of age. Brain *Ccdc42* expression was present in 8 day old mice prior to testes expression. (A and B) β-Actin is used as a template control. (C) β-galactosidase staining assay for *Ccdc42*-β-gal reporter in the testes and brain. β-galactosidase activity is present in maturing spermatids in the adluminal region of the seminiferous tubule of $Ccdc42^{Het}$ testes. $Ccdc42^{KO}$ sections reveal staining in malformed spermatids. $Ccdc42^{WT}$ testes are a negative control for staining. Purkinje cells of the cerebellum stain positive for β-galactosidase activity. Sections counterstained with Fast Red. All scale bars 60 μm.

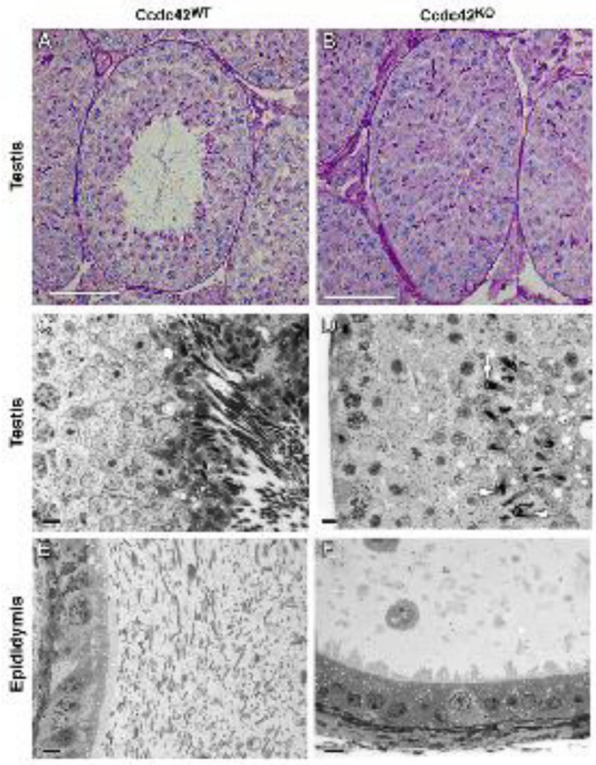

Figure 3. Testicular and epididymal phenotypes in Ccdc42^{KO} mice

(A) Periodic acid-Schiff and hematoxylin staining of testes cross sections from 8 week old control (*Ccdc42^{WT}*) and mutant (*Ccdc42^{KO}*) mice. *Ccdc42^{KO}* mice display both an absence of a lumen and spermatid flagella. Scale bars 60 μm. (C) High magnification plastic section through a seminiferous tubule stained with toluidine blue. Mature spermatids are released into the lumen during spermiation in *Ccdc42^{WT}* mice. (D) Spermiation stage in the seminiferous tubule of *Ccdc42^{KO}* mice. Arrows indicate mature spermatids with abnormal shaped heads. No flagella tails are observed in *Ccdc42^{KO}*. (E) Epididymal duct in a *Ccdc42^{WT}* mouse with flagellated sperm. (F) Epididymis from an age matched *Ccdc42^{KO}* mouse devoid of sperm contains only cellular debris. (C–F) Scale bars 5 μm.

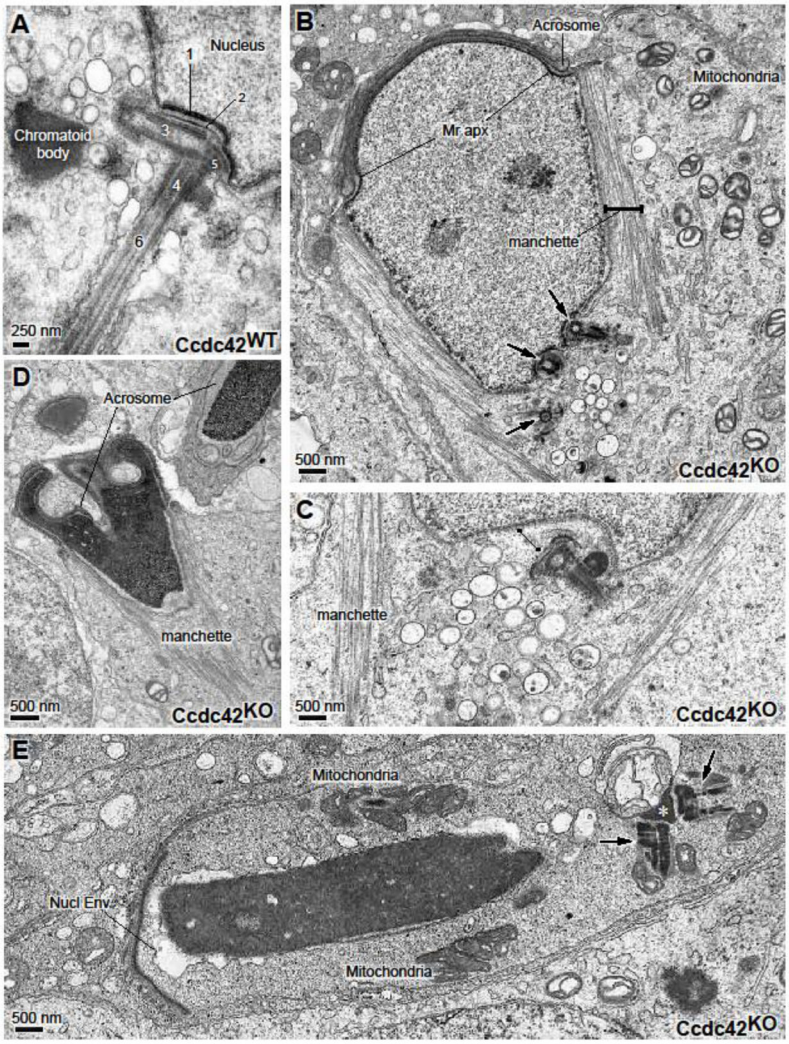

Figure 4. Morphological defects in Ccdc42^{KO} spermatids

(A–E) Transmission electron micrographs of spermatids. (A) The HTCA in an elongating spermatid of a *Ccdc42^{WT}* mouse. The following are indicated: (1) nuclear implantation fossa, (2) capitulum, a dense plate facing the implantation fossa, (3) proximal centriole, (4) distal centriole, the emerging site of the, (6) axoneme, (5) banded collar surrounding the HTCA, A typical chromatoid body and adjacent vesicles are also visible. (B) Elongating spermatid of a *Ccdc42^{KO}* mouse. Three HTCAs (arrows) are present in this section, surrounded by numerous particle-filled vesicles. Two HTCAs are anchored to implantation fossae, the other HTCA is separate from the nucleus. The microtubules of the manchette are present, but no microtubule axonemes are observed from any of the HTCAs. The marginal ring of the acroplaxome (Mr apx) and the associated acrosome are present but mitochondria are dispersed. There is no indication of outer dense fiber assembly. (C) A structurally normal looking HTCA from a mutant mouse is dissociated from its anchoring site and has no axoneme. The microtubules of the manchette and adjacent vesicles in the elongating spermatid of a *Ccdc42^{KO}* mouse appear normal. (D) A *Ccdc42^{KO}* condensed spermatid nucleus with abnormal nuclear folding. The manchette is still present. (E) A nearly mature

spermatid in the *Ccdc42*^{KO} with two HTCAs (arrows) attached to a fragment of nucleus (*). There is no evidence of flagellogenesis. The nuclear envelope (Nucl Env) is detached from the condensed chromatin and clusters of mitochondria can be seen.

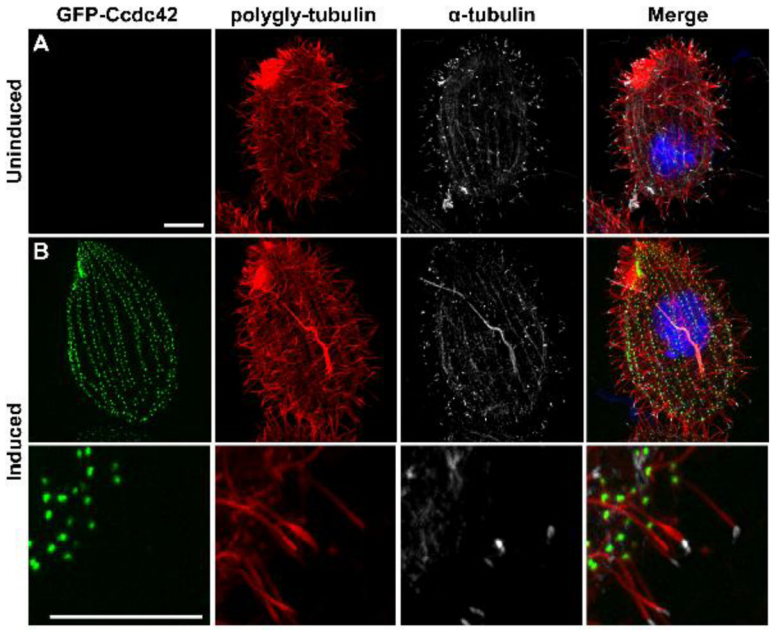

Figure 5. GFP-Ccdc42 localizes to the base of cilia in transgenic Tetrahymena thermophila

(A) In the uninduced state, no GFP signal is detected in transgenic GFP-Ccdc42 cells. Cilia axonemes (red) have been labeled with a polyglycylated tubulin (2302) antibody. Cilia tips (white) have been labeled with an α-tubulin antibody (12G10). (B) Two hours after the addition of $^{CdCl}2$ to induce transgene expression, GFP-Ccdc42 (green) can be seen at the bases of the cilia. Nuclei have been labeled with Hoechst. Scale bar is 30 μm. Higher magnification images are shown in the bottom panels.

Table 1

Fertility of Ccdc42^{WT} and Ccdc42^{KO} mice

	WT♂ x WT♀	WT♂ x KO♀	KO♂ x WT♀
Matings	7	7	12
Fertility (Litters/plug)	0.86	0.86	0
Mean Litter Size	7.8 ± 0.4	6.3 ± 0.6	0

Males and females (8 – 12 weeks of age) from both Ccdc42^{WT} and Ccdc42^{KO} mice were tested for fertility (number of litters per copulatory plug) and for average litter size. No significant difference was found in the mean litter size between Ccdc42^{WT} and Ccdc42^{KO} females ($p=0.1487$; Dunn's post hoc after Kruskal-Wallis). In contrast, Ccdc42KO males were completely sterile ($p<0.01$). Copulation was determined by the presence of a vaginal plug the morning after a mating was established.